



Electromagnetic Field Study

Electromagnetic field measurements: environmental noise report.

Prepared by
Michael Slater, Science Applications International Corporation
Dr. Adam Schultz, consultant
Richard Jones, ENS Consulting
on behalf of Oregon Wave Energy Trust

This work was funded by the Oregon Wave Energy Trust (OWET). OWET was funded in part with Oregon State Lottery Funds administered by the Oregon Business Development Department. It is one of six Oregon Innovation Council initiatives supporting job creation and long-term economic growth.

Oregon Wave Energy Trust (OWET) is a nonprofit public-private partnership funded by the Oregon Innovation Council. Its mission is to support the responsible development of wave energy in Oregon. OWET emphasizes an inclusive, collaborative model to ensure that Oregon maintains its competitive advantage and maximizes the economic development and environmental potential of this emerging industry. Our work includes stakeholder outreach and education, policy development, environmental assessment, applied research and market development.

Record of Revisions

Revision	Date	Section and Paragraph	Description of Revision
Original	March 2011	All	Initial Release

TABLE OF CONTENTS

1. EXECUTIVE SUMMARY	4
2. INTRODUCTION	6
2.1 REPORT ORGANIZATION.....	7
2.2 METHODOLOGY	7
3. INSTRUMENTATION SETUP – IN SITU CABLE DEPLOYMENT	8
3.1 MAGNETIC FIELD SENSORS	9
3.2 ELECTRIC FIELD SENSORS.....	10
3.3 DATA RECORDER	11
3.4 CALIBRATION	12
4. IN-SITU CABLE DEPLOYMENT.....	13
4.1 DESCRIPTION.....	14
4.2 ELECTRIC FIELD SENSORS.....	15
4.3 MAGNETIC FIELD SENSORS	15
4.4 DATA ACQUISITION SUMMARY	16
5. DATA PROCESSING AND ANALYSIS	17
5.1 DATA PROCESSING.....	17
5.2 SPECTRAL ANALYSIS	26
6. ACTIVE SOURCE VERIFICATION DEPLOYMENT.....	29
6.1 METHODOLOGY	30
6.2 DEPLOYMENT.....	30
6.3 DATA ANALYSIS	30
7. DATA SUMMARY	34
8. DISCUSSION.....	35
8.1 MEASUREMENT RELIABILITY	35
8.2 MEASUREMENT AFFORDABILITY	35
8.3 MEASUREMENT REPEATABILITY	36
9. CONCLUSIONS AND RECOMMENDATIONS.....	36
9.1 SUMMARY OBSERVATIONS	36
9.2 APPLICATION OF THE TECHNOLOGY.....	37
9.3 ADDITIONAL TECHNICAL RECOMMENDATIONS.....	37
APPENDIX A – ACRONYMS	40
APPENDIX B – PROBE CALIBRATION LOGS.....	41
APPENDIX C – REFERENCE DOCUMENTS	45

TABLE OF FIGURES

FIGURE 1 - PROTOTYPE INSTRUMENT ON DECK OF TEST VESSEL PRIOR TO DEPLOYMENT	8
FIGURE 2 - UNIAXIAL MAGNETIC FIELD SENSOR, SHOWN WITH NON-METALLIC PRESSURE VESSEL	9
FIGURE 3 - ELECTRIC FIELD PROBES AND WET-MATE INTERCONNECT CABLE	11
FIGURE 4 - SIX-CHANNEL DATA RECORDER ASSEMBLY 'STACK'	12
FIGURE 5 - MAGNETIC SENSOR UNDERGOING MAGNETIC CALIBRATION	13
FIGURE 6 - SENSOR LOCATIONS DURING DEPLOYMENT	14
FIGURE 7 - DEPLOYMENT OF PROBE ASSEMBLY AT IN-SITU TEST SITE	16
FIGURE 8 - VIEW OF LOC#3 MARKER BUOYS LOOKING TOWARD CABLE LANDING ZONE	16
FIGURE 9 - E-FIELD SPECTROGRAM IMAGE, SENSOR E1, HORIZONTAL	19
FIGURE 10 - E-FIELD SPECTROGRAM IMAGE, SENSOR E2, HORIZONTAL.....	20
FIGURE 11 - E-FIELD SPECTROGRAM IMAGE, SENSOR E3, VERTICAL	22
FIGURE 12 - B-FIELD SPECTROGRAM IMAGE, SENSOR M1, HORIZONTAL	23
FIGURE 13 - B-FIELD SPECTROGRAM IMAGE, SENSOR M2, HORIZONTAL	24
FIGURE 14 - B-FIELD SPECTROGRAM IMAGE, SENSOR M3, VERTICAL	25
FIGURE 15 - REPRESENTATIVE SIGNAL-TO-NOISE ANALYSIS, MAGNETIC SPECTRA, 60 HZ	27
FIGURE 16 - REPRESENTATIVE B-FIELD MAGNETIC SPECTRUM, VERTICAL, 1 HZ BANDWIDTH	28
FIGURE 17 - B-FIELD SPECTROGRAM IMAGE, SENSOR M3, VERTICAL	31
FIGURE 18 - REPRESENTATIVE B-FIELD MAGNETIC SPECTRUM, VERTICAL, 1 HZ BANDWIDTH	32
FIGURE 19 - B-FIELD RELATIVE MAGNITUDE, VERTICAL, 256 HZ BAND (1 HZ BANDWIDTH)	33

TABLE OF TABLES

TABLE 1 - SENSOR LOCATIONS DURING IN-SITU CABLE DATA COLLECTION	15
TABLE 2 - E-FIELD ELECTRODE SPACING	15
TABLE 3 - ELECTRIC FIELD SUMMARY, AC POWER FREQUENCIES, SPECTRUM LEVEL	28
TABLE 4 - MAGNETIC FIELD SUMMARY, AC POWER FREQUENCIES, SPECTRUM LEVEL.....	29

1. EXECUTIVE SUMMARY

The Oregon Wave Energy Trust (OWET) commissioned this study to develop protocols and methods to achieve affordable, reliable, and repeatable electromagnetic (EM) measurements in the near-shore environment. This report presents the calibration and measurement results from a prototype EM instrument deployed near a submarine power cable in a representative undersea environment. The data demonstrate that electromagnetic fields (EMF) are indeed present and measureable even from an energized cable of modest electrical capacity. Higher energy cables carrying more electrical current would undoubtedly produce higher EM signatures, which would be observable at greater distances than were measured by the prototype instrument.

As part of this project, the team designed and constructed an instrument to demonstrate that available components could be assembled to achieve basic measurement objectives. The stand-alone EM instrument was comprised of tri-axial electric and magnetic field sensors capable of measuring the relevant bandwidth of interest, and was outfitted with a multi-channel sampling and storage capability to acquire EMF data for processing and analysis. The instrument was deployed in-situ at two different near-shore marine environments, and acquired EM field data near an operating submarine power cable-of-opportunity to show the efficacy of the system to quantify EM emanations due to the influence of the power cable within the environment. As part of this activity, the instrument was calibrated in a laboratory to ensure a valid and repeatable methodology for measurements. Results of the instrument deployments are presented, including analyses of EM spectral processing. Data acquired clearly showed the presence of strong electric (E-field) and magnetic (B-field) power line frequencies and harmonics (namely 60 Hz, 180 Hz, 300 Hz, and 420 Hz discrete lines) near the power cable, which dissipated as the instrument was moved away from the cable, as expected. EM fields created by submarine cables of a commercial capacity (in the megawatt range) would be expected to create much stronger fields than those measured during this study, and would be detected at further distances.

The affordability, reliability, and repeatability objectives of the study were demonstrated. Modeling, calibration, measurement, and processing protocols and techniques identified within this study serve to advance the science of marine EM measurements in coastal waters, and promote a standardized methodology that is both reliable and repeatable.

The following summary conclusions and recommendations are made:

1. Substantial published data is lacking on observed effects to marine species from EM fields at power frequencies (60 Hz and harmonics). Application of equipment and techniques documented within this study could easily be adapted to provide repeatable, quantifiable EM field data to ensure that observable conclusions are based on valid data sets.

Recommendation: Conduct additional biological study to better understand and quantify observed effects to biota from man-made EMF. Apply equipment and techniques developed in this study in support this of biological research.

2. Due to the limited scope of the study, the long-term temporal variability of naturally occurring EM fields was not quantified in terms of range or extent. Longer term monitoring or periodic sampling would provide better insight into the naturally occurring environment, as well as that of operating energy generating facilities. Scientific documentation of concurrent conditions over longer time horizons (weeks, months, seasons) will add to the physical understanding, and hence, biological understanding of measured EM fields.

Recommendation: Conduct long-term monitoring with energized cables. As part of monitoring, collect electrical and physical data to correlate measured levels to physical phenomena.

3. Modeling and predictions of E- and B-field strengths in the coastal environment are strongly dependent on local conditions, including the underlying geology. In particular, local conditions substantively affect longer-range propagation of EM fields. The existing modeling framework together with a larger set of physical measurements of in-situ data using technologies demonstrated within this study can account for these phenomena and lead to a better understanding and predictions for impacts to potential wave energy sites.

Recommendation: Evaluate and improve existing modeling capabilities with measured data at wave energy sites. Consider performing this activity while concurrently monitoring energized cables along Oregon's coast.

2. INTRODUCTION

The major objective of this project was to demonstrate an ability to achieve affordable, reliable, repeatable EMF measurement protocols in support of wave and tidal energy technology development and deployment. As such, this report was prepared to describe the prototype instrumentation fabricated with affordable and available components, calibration results to provide the basis for repeatability, and a data summary of the ambient background and energized power cable measurements conducted during at-sea measurement deployments.

The results provided in this report are the culmination of a series of studies to investigate methods, protocols, and other significant input parameters for establishing reliable, repeatable, and affordable EM measurements at wave project sites. The following reports were prepared to investigate, analyze, and report on current near-shore EMF knowledge base, to research state-of-the-art and available technologies in measurement approaches and equipment, and prepared to review measurement physics, including sources and modes of EM generation and propagation. Methods were assessed and summarized, with alternatives and recommendations provided to achieve the project objectives. Data for these reports were obtained through literature reviews, market surveys, computational activities, and laboratory and field tests.

- Effects of Electromagnetic Fields on Marine Species: A Literature Review, report 0905-00-001
- Estimated Ambient Electromagnetic Field Strength in Oregon's Coastal Environment, report 0905-00-002
- The Prediction of Electromagnetic Fields Generated by Wave Energy Converters, report 0905-00-003
- EMF Synthesis: Site Assessment Methodology, report 0905-00-004
- EMF Measurements: Data Acquisition Requirements, report 0905-00-005
- EMF Measurements: Instrumentation Configuration, report 0905-00-006
- The Prediction of Electromagnetic Fields Generated by Submarine Power Cables, report 0905-00-007
- Ambient Electromagnetic Fields in the Near shore Marine Environment, report 0905-00-008
- Trade Study: Commercial Electromagnetic Field Measurement Tools, report 0905-00-009
- EMF Measurements: Field Sensor Recommendations, report 0905-00-010
- Summary of Commercial EMF Sensors, report 0905-00-012

These reports are available from the Oregon Wave Energy Trust, <http://www.oregonwave.org/>. Results from these studies were combined to prepare the prototype instrument to demonstrate that near-shore EM field measurements could be reliably and affordably obtained at coastal project sites.

2.1 Report Organization

This report contains seven primary sections, and includes supporting appendices. The first sections contain the executive summary and introduction, and provide the project background. Setup of the prototype instrument is described in Section 3. The first deployment is described in Section 4, with the data processing and analysis results from that deployment discussed in section 5. Section 6 describes methods and results from a deployment of the instrument near an energized pipeline in Newport Bay, Oregon. A discussion of the results of the study are provided in Section 8, with conclusions and recommendations presented in Section 9. Appendix A contains an acronym list, and Appendix B contains calibration logs. Reference documents are listed in Appendix C.

2.2 Methodology

A prototype EM probe was constructed to demonstrate that basic, low cost instrumentation could provide affordable, reliable, and repeatable near-shore EM measurements in the marine environment. While available, commercial wideband electric and magnetic field measurement systems are expensive. Further, commercially available magnetic systems generally do not extend up into the kHz frequency range. Thus, the use of magnetic sensors in this study press the current commercial technology above that which is typically available.

As part of this study, a low cost prototype instrument was assembled to demonstrate that such measurements could be obtained with a modest tool. After assembly, the instrument was calibrated in a laboratory, and then deployed to assess the naturally occurring magnetic and electric fields and the emanated electric (E) and magnetic (B) fields from a three-phase AC submarine power cable, and also from an energized submarine pipeline. This report describes the basic instrument and data collection parameters, provides calibration data, and discusses measured results obtained during the demonstration deployments.

3. INSTRUMENTATION SETUP – IN SITU CABLE DEPLOYMENT

The instrument was constructed using available components (see Figure 1) following the recommendations provided in an earlier phase of this study (reference (a)). Tri-axial arrangements of magnetic and electric field sensors were made to obtain orthogonal measurement of B-field and E-field parameters across the frequency range of primary interest, from a few tens of milli-Hz to approximately 500 Hz. The instrument was fully self-contained, with a six-channel high-resolution recording system implemented to receive, sample, and store data for subsequent processing, and a DC battery supply to provide system and sensor power for the duration of the deployment and to avoid any potential AC signal contamination.

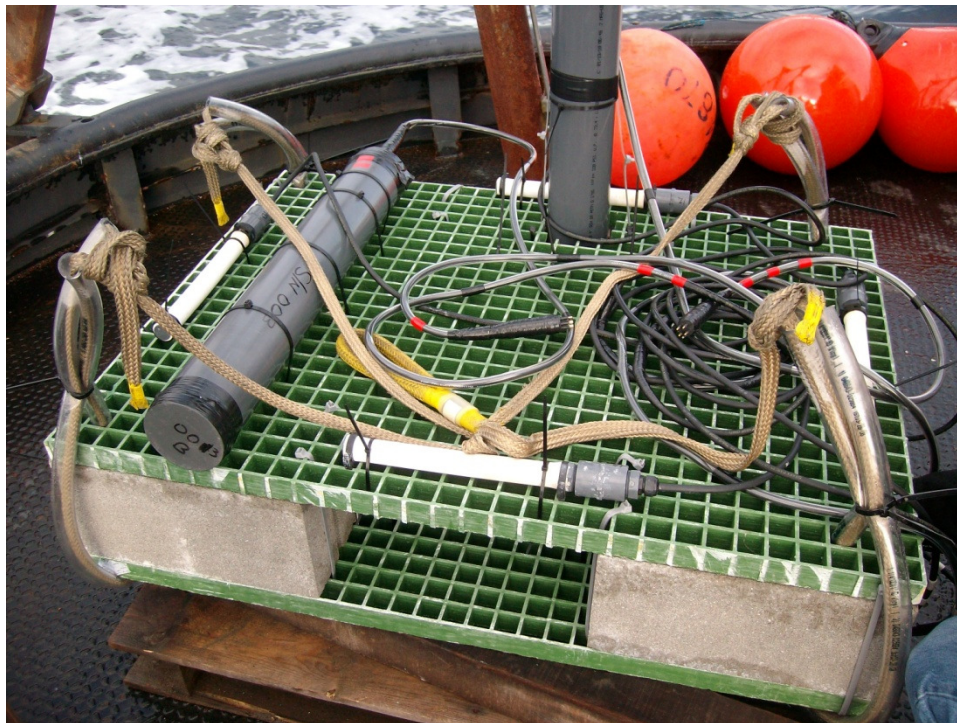


Figure 1 - Prototype instrument on deck of test vessel prior to deployment

Due to the sensitivity of the instruments, wherein motion can induce erroneous measurements by increasing the self-noise level of the instrument, a stable platform was required to minimize movement on of the probe during deployment. Thus, an open platform was fabricated using common construction materials (fiberglass, PVC, concrete, vinyl tubing, plastic cable ties, etc.) to mount the sensors and the instrumentation/battery pack. A deliberate use of non-metallic components minimized possible spurious influence of the recorded data due to the proximity of

electrical or magnetic properties of metallic components. During deployment, the probe platform was lowered to the ocean floor, with a small float attached to mark the instrument for recovery. The overall in-air weight of the instrument was approximately 250 lbs, including concrete weights.

3.1 Magnetic Field Sensors

Induction coil type magnetic sensors were used to sense magnetic fields. Uniaxial ANT-2 antennas from Zonge International, Inc. (Zonge) utilizing a metallic core and an overall length of 18 inches were packaged within pressure vessels constructed from PVC (see Figure 2). The specific design of this particular was well suited to the prototype instrument, which was a result of joint development by Zonge and the Oregon State University (OSU) as part of the National Science Foundation funded National Geoelectromagnetic Facility. Thus, while not completely a commercial component, these sensors were made available to this study via OSU and Zonge in advance of commercial release.



Figure 2 - Uniaxial magnetic field sensor, shown with non-metallic pressure vessel

The probes provided a basic sensitivity of .1V/nT (see Appendix B), and was flat to within 1 dB over the range of 30 Hz to 50 kHz. The low-frequency regime of this sensor rolled off below

30 Hz, with a useable response extending below 1 Hz. Sensors provided a low impedance differential output, and were wired from each sensor output to the data recorder using balanced, shielded cable. During assembly and testing, it was noted that minor movement of the sensors clipped the input of the data recorder (± 2 volts). Differential attenuators (20 dB) were used on the sensor output to limit the output voltage to optimize the available dynamic headroom on the recorder once deployed without clipping the inputs. Pressure vessels were rated for a depth of 250 feet in seawater, and tested in a pressure tank at 130 psi (equivalent to 290 feet of seawater) prior to deployment. Commercial wet-mate pluggable connectors were used to wire the sensors to the recording unit.

3.2 Electric Field Sensors

Low-cost electric field sensors were fabricated in pairs using a lead-lead chloride formulation. The inspiration for the basic electrode design was derived from Webb et al. (reference (b)), who used a silver-silver chloride (Ag-AgCl) sensor chemistry. To keep the sensors affordable, a lead-lead chloride (Pb-PbCl₂) sensor chemistry was adopted for the prototype after Petiau (reference (b)). In our approach, commonly available components were prepared and assembled to achieve very low impedance to seawater, thus reducing the effective sensor noise floor. A diatomaceous earth mixture was prepared to encase the metallic electrodes within a porous sleeve to allow ionic exchange with the surrounding seawater (see Figure 3). This process resulted in probes with a resistance of only a few ohms using electrodes approximately 12 inches in length; electrodes were matched in pairs to minimize DC bias, a known condition common to metallic electrodes. Electrode pairs were cabled to differential inputs of the data recorder.



Figure 3 - Electric field probes and wet-mate interconnect cable

3.3 Data Recorder

Single-channel analog-to-digital recording boards were assembled into a six-channel “stack” to record three each electric field and magnetic field channels (see Figure 4). Each recorder board was configured for a single channel with differential input, and 32 bits of digital resolution provided a wide dynamic range for recording and low system noise floor. The recorder operated as a state machine, and initiated recording upon power-up and synchronization. One board operated as the master, and all boards were synchronized to within one sample to the master board. Sampling rate was set to 1024 samples per second (1024 Hz), providing a useable measurement bandwidth of 512 Hz. Upon deployment, data were synchronized and continuously recorded to microSD formatted memory cards.

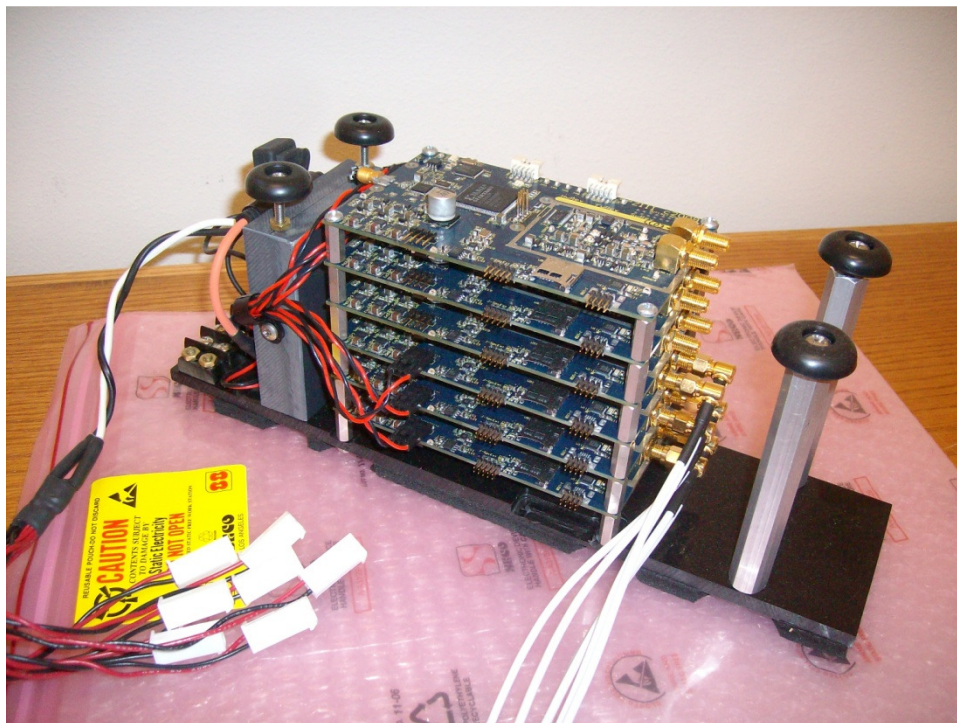


Figure 4 - Six-channel data recorder assembly 'stack'

3.4 Calibration

Calibration followed the basic procedure outlined in reference (d), including the use of a 12-foot long, 10" diameter calibration coil with 144 wraps (see Figure 5). Using this coil and a precision resistor, the electrical current passing through the coil was measured with a 6.5 digit calibrated voltmeter. The magnetic field strength within the coil was then computed. The output of each magnetic sensor was measured using a narrowband spectrum analyzer and compared to the manufacturer's specifications for instrument sensitivity. Calibration results are provided in Appendix B for the three magnetic sensors used during the deployment, which shows excellent agreement with the manufacturer's specification over a wide range of frequencies, from 30 Hz to over 50 kHz. A cursory linearity analysis was done showing that the magnetic sensors were flat over the range tested, from 1 nT to over 100 nT, with a useable noise floor of better than 2 pT/ $\sqrt{\text{Hz}}$ at 60 Hz.



Figure 5 - Magnetic sensor undergoing magnetic calibration

Electrical calibration of the data recorder was conducted by injecting a known AC voltage into the front-end of each data recorder channel and measuring the output. A single-frequency sine wave was generated using an arbitrary waveform generator and injected into each channel. Root mean square (RMS) levels were measured using a calibrated voltmeter, which verified that the output was within the manufacturer's specifications.

4. IN-SITU CABLE DEPLOYMENT

After seeking a suitable AC power cable in the oceanic, salt-water environment along the Oregon coast and finding none, a representative cable was located in a controlled Pacific Coast environment, with access provided by a cooperating entity, which provided nominal cable operating parameters during field measurements. The governing agreement between SAIC and the cooperating entity permitted distribution of the experimental results and protected specifics about the entity's operations.

A local test vessel outfitted with an A-frame was contracted to deploy and recover the probe assembly. The probe was shipped to an in-port location, assembled, and staged on the test vessel the day prior to the measurement period. Approximately four hours were required to unpack, assemble, and prepare the probe for data recording. New batteries were fitted, sensors were positioned on the frame, and the sensing and recording equipment was verified to be operational. On the morning of May 28, 2010, the probe was loaded onto the test vessel, which transited to the measurement site.

4.1 Description

After the data recording was started, the test vessel maneuvered to each measurement location and the probe was lowered to the bottom and marked with surface marker buoys. During the measurement period, the test vessel maneuvered away from each probe location to a position greater than 1 km away to minimize any potential interference to the measured data. The probe recorded data continuously during the entire deployment. Measurement locations are shown in Figure 6. Locations were selected to provide a comparable suite of measurement conditions to determine the spatial dependence of the expected EM fields at various distances from an energized cable. Care was taken to stay away from the restricted cable right-of-way to avoid disturbing the cable itself. The closest location was less than 75 meters from the cable itself, and the furthest location was up to one half kilometer (500 meters) away (see Table 1). All measurement positions were located at approximately the same depth (22 to 24 meters of water). Weather conditions during the measurement period were calm. Wave swell amplitude was less than 1 foot, and observed tidal currents were minimal.

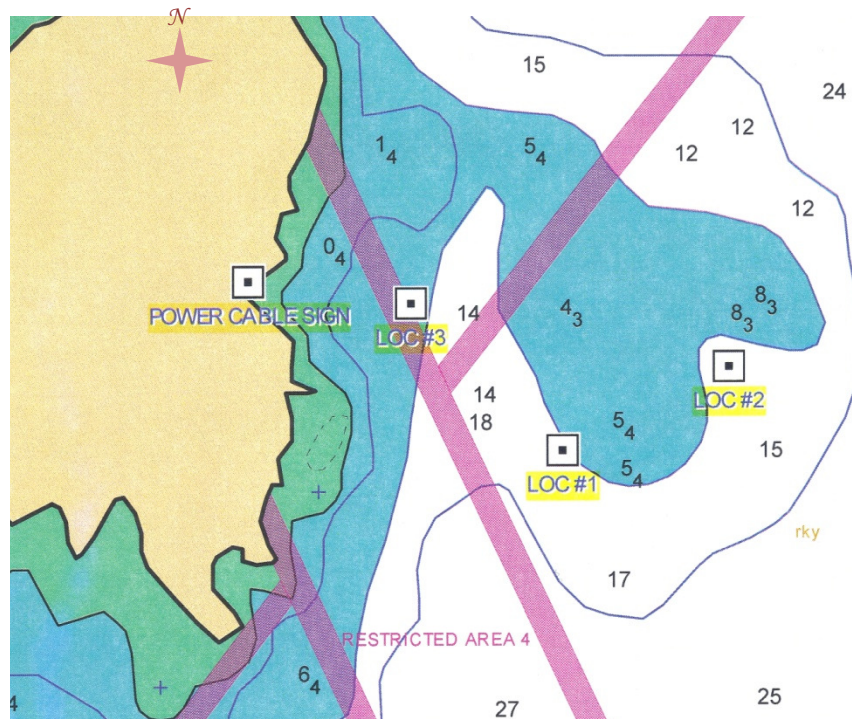


Figure 6 - Sensor locations during deployment

Table 1 - Sensor locations during in-situ cable data collection

Sensor Location	Approximate Distance to Cable (meters)	Water depth (meters)
LOC#1	150 to 200	23
LOC#2	400 to 500	24
LOC#3	50 to 75	22

4.2 Electric Field Sensors

The electric field electrode pairs were mounted to the probe platform on the same orthogonal axes as the magnetic sensors. The spacing varied with each pair, based on the physical dimensions of the probe platform (see Table 2).

Table 2 - E-field electrode spacing

Sensor ID	Orientation	Separation
E1	Horizontal	1.07 meters (42")
E2	Horizontal	.80 meters (31.5")
E3	Vertical	.47 meters (18.6")

4.3 Magnetic Field Sensors

Three induction coil magnetic sensors were encased in PVC pressure vessels and mounted in an orthogonal configuration, two each in the horizontal plane at right angles, and one vertically (see Figure 7). Orthogonal mounting allowed relative comparison of magnetic field strength based on spatial orientation to the energized cable.



Figure 7 - Deployment of probe assembly at in-situ test site



Figure 8 - View of LOC#3 marker buoys looking toward cable landing zone

4.4 Data Acquisition Summary

Six channels were continuously recorded for a period of 4 hours, 53 minutes. Valid data were recorded at each of three locations, with a minimum of one hour at each site. At the end of the recording period, the probe was recovered on deck, and the memory cards removed for processing and analysis. Approximately 330 megabytes of data were recorded for each channel,

with an overall aggregate amount of 2 gigabytes. Files were read and converted into a MATLAB[®] compatible data format.

5. DATA PROCESSING AND ANALYSIS

5.1 Data Processing

Data were recorded on each channel using a 1024 sampling frequency, thus providing a useable frequency bandwidth of 512 Hz. Time series data were calibrated using measured calibration values for each channel, and then high-pass filtered and processed using short-time Fourier transforms to provide spectrum level (1 Hz bandwidth) signatures over the measurement period. Time-frequency spectrograms were computed for each channel over the 4 hour, 53 minute measurement duration to provide a visual representation of the complete recording period. The first thirty-three minutes of each recorded channel represent instrument setup and test vessel maneuvering to the first measurement location. The probe was on deck for this period. It was observed that prior to deployment, relatively high levels of both electric and magnetic fields were recorded which were attributed to sensor motion, and relative proximity to the test vessel equipment, including engines and generator, and electrical circuitry. The set-up and maneuvering period is shown in the approximate period marked from the 0 to 2000 second timescale in the figures.

The recording time of each of three measurement locations is annotated on each figure. Time at Location #1 was 90 minutes, spanning the 2000 to 7388 second timescale. The probe was located from 150 to 200 meters from the energized cable, which was operating at a nominal voltage of 12.7 kV, and carrying between 8 and 10 amperes of AC current during the measurement period.

The second location, marked from nominally 8000 to 12000 seconds, represents approximately 66 minutes, of recording time. The wide, prominent vertical yellow-green bands in Figures 9, 10, and 11 show periods of time during which the probe was recovered from the bottom, and the test vessel maneuvered to the new location and re-deployed the probe on the bottom.

Location #3 represented the closest measurement to the energized AC cable. Data were recorded approximately 70 minutes at this location, at an estimated distance between 50 and 75 meters from the cable. Resulting spectrogram images for each channel presented in Figures 9 through 14, using a logarithmic decibel scale to represent signal amplitude. Recording time begins on the left-hand side of each chart, and progresses to the right-hand side, with the time-scale given in seconds from the beginning of the data recording.

As expected, both electric and magnetic signatures at the fundamental power frequency (line voltage, 60 Hz) and higher order harmonics (180, 300, and 420 Hz) from the energized cable were stronger near the cable, and diminished in amplitude away from it. Theory predicts that the electric field emanates radially from a cable, and is orthogonal to the magnetic field. Thus, strongest electric fields were expected in the horizontal dimension pointing “away” from the cable, and essentially zero parallel to the cable in either the vertical or horizontal orientation. This can be seen in Figures 9 and 10, wherein power frequency harmonics were observed in the horizontal direction (especially at Location #3), and they were notably absent in the vertical direction.

The dominant 60 Hz line in the horizontal dimension was evident at Locations #1 and #3, showing that the field was detected up to 200 meters from the cable. Multiple odd-harmonics of 60 Hz were also seen at Location #3 (180 Hz, 300 Hz, and 420 Hz) within 75 meters from the cable. The presence of 180 Hz energy and higher order odd harmonics from the cable indicate that the electrical power waveform was not purely sinusoidal, and was likely distorted. A few discrete, time variant frequencies were noted in the data set from an unknown source, which are annotated on the charts.

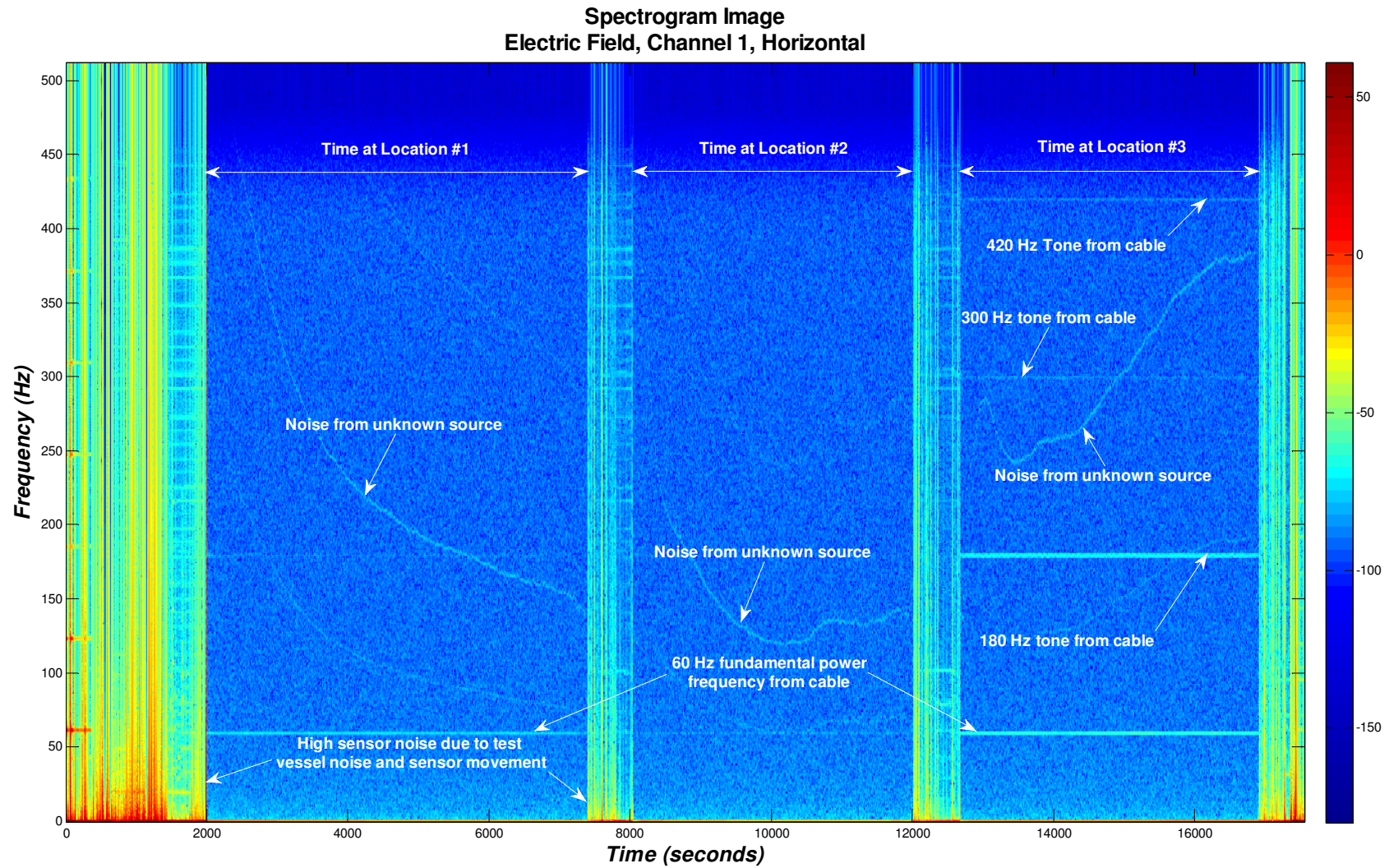


Figure 9 - E-field Spectrogram Image, Sensor E1, Horizontal

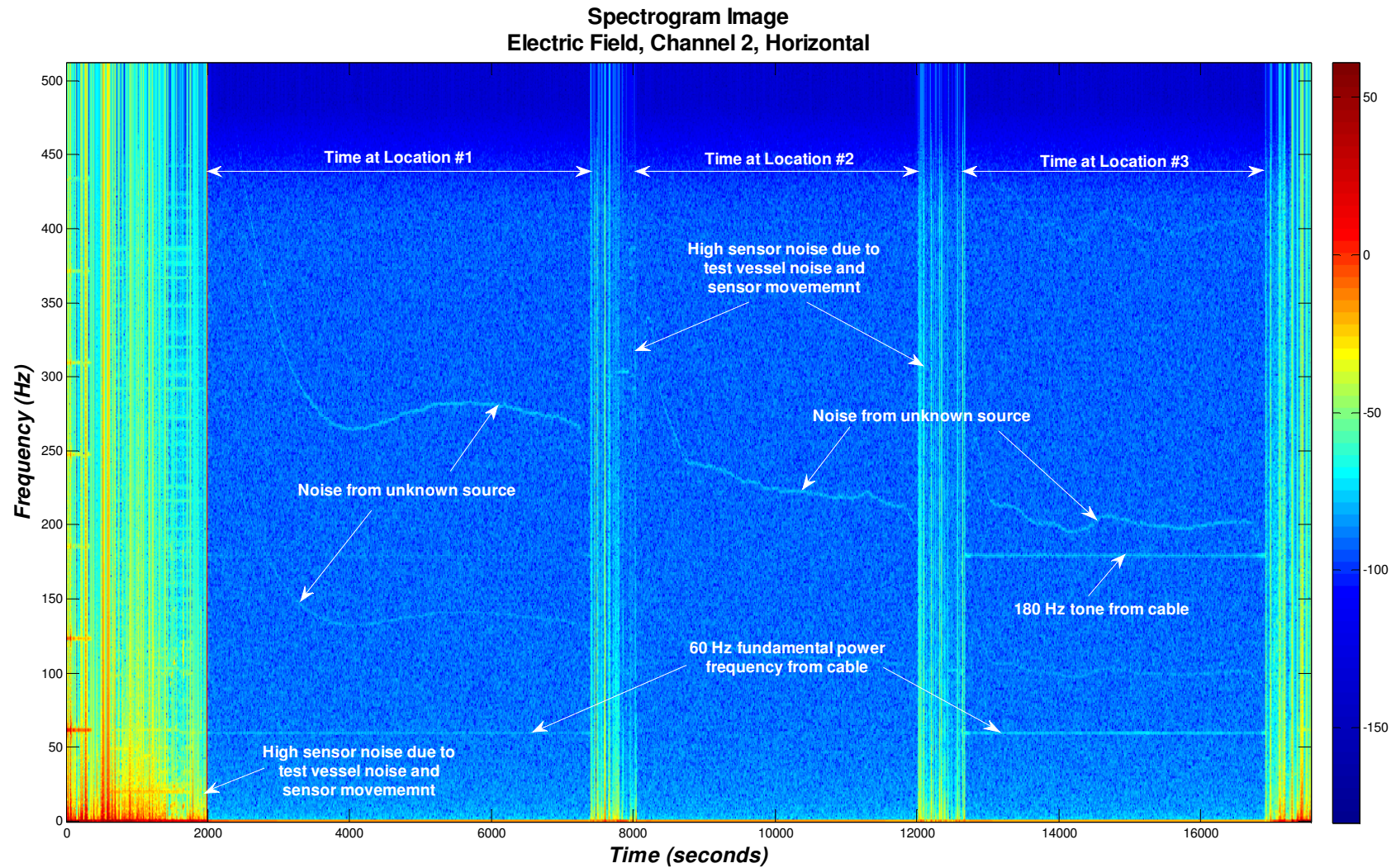


Figure 10 - E-Field Spectrogram Image, Sensor E2, Horizontal

In the vertical direction, the measured electric field was non-descript at all measured locations, and in particular AC power cable harmonics were not readily apparent (see Figure 11) with a nominal continuum level of less than $100 \mu\text{V/m}$. The addition of low-noise preamplifiers would serve to reduce the level of background noise in the measured spectra such that power harmonics might be more easily detected, but it was clear that this dimension was less important for the assessment of power cable frequencies as predicted by electrical field theory. It should be noted that the cable measured was carrying approximately 10 amps of AC current, which would be substantially lower than the level of current expected to be carried by marine energy power export cables, which might range from perhaps 100 amps to over 1000 amps of AC current. Since the induced electric field strength at a given distance from a cable is directly proportional to the current being carried in the cable, it is likely that received levels by the probe near such power cables would provide a much stronger, and thus more detectable signal than those measured during the in-situ tests presented herein.

Figures 12 and 13 show the horizontal magnetic fields observed during the measurement period, and Figure 14 shows the resultant B-field in the vertical dimension. Theory predicts that magnetic fields around a power cable flow around the cable in a circumferential manner, thus in generalized homogeneous environment, an energized cable will product “right-hand-rule” responses to the magnetic field surrounding the cable. All things being equal, no vertical component is expected when directly over an energized cable, and when a cable is crossed, the polarity of the vertical B-field reverses. Likewise, the intensity of the horizontal B-field increases monotonically and symmetrically as the cable is approached from either side. In practice it is unlikely to attain perfectly aligned conditions to achieve theoretical prediction, but in general, predictive theory provides the basis for understanding actual results. So, for any general location in the real world, both vertical and horizontal components to the B-field may be present. In the case of the data obtained during this deployment, sensors were located at some perpendicular distance (greater than 50 meters) from the energized cable, thus the magnitude of the vertical component were expected to be more significant than horizontal components of the B-field vector.

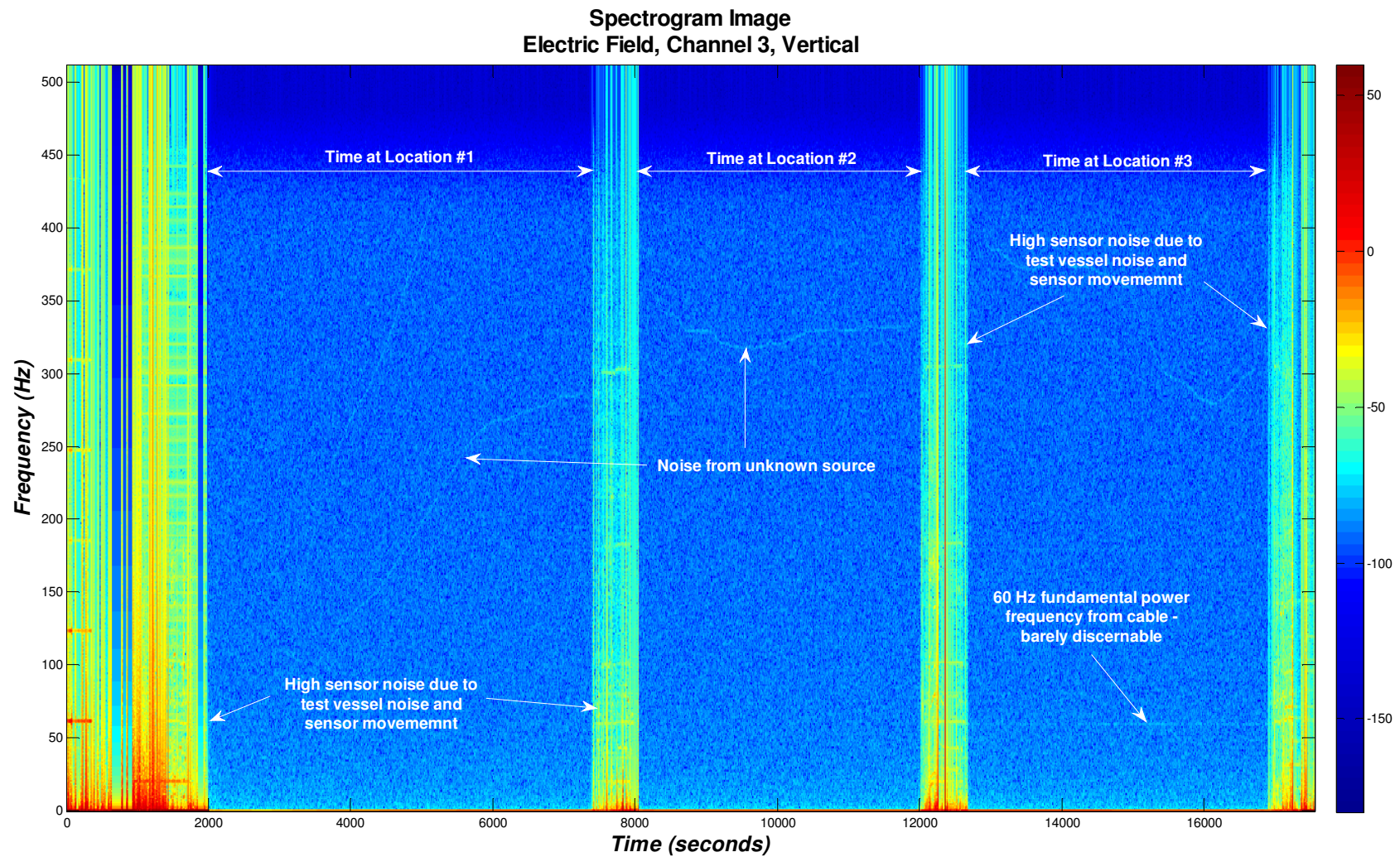


Figure 11 - E-Field Spectrogram Image, Sensor E3, Vertical

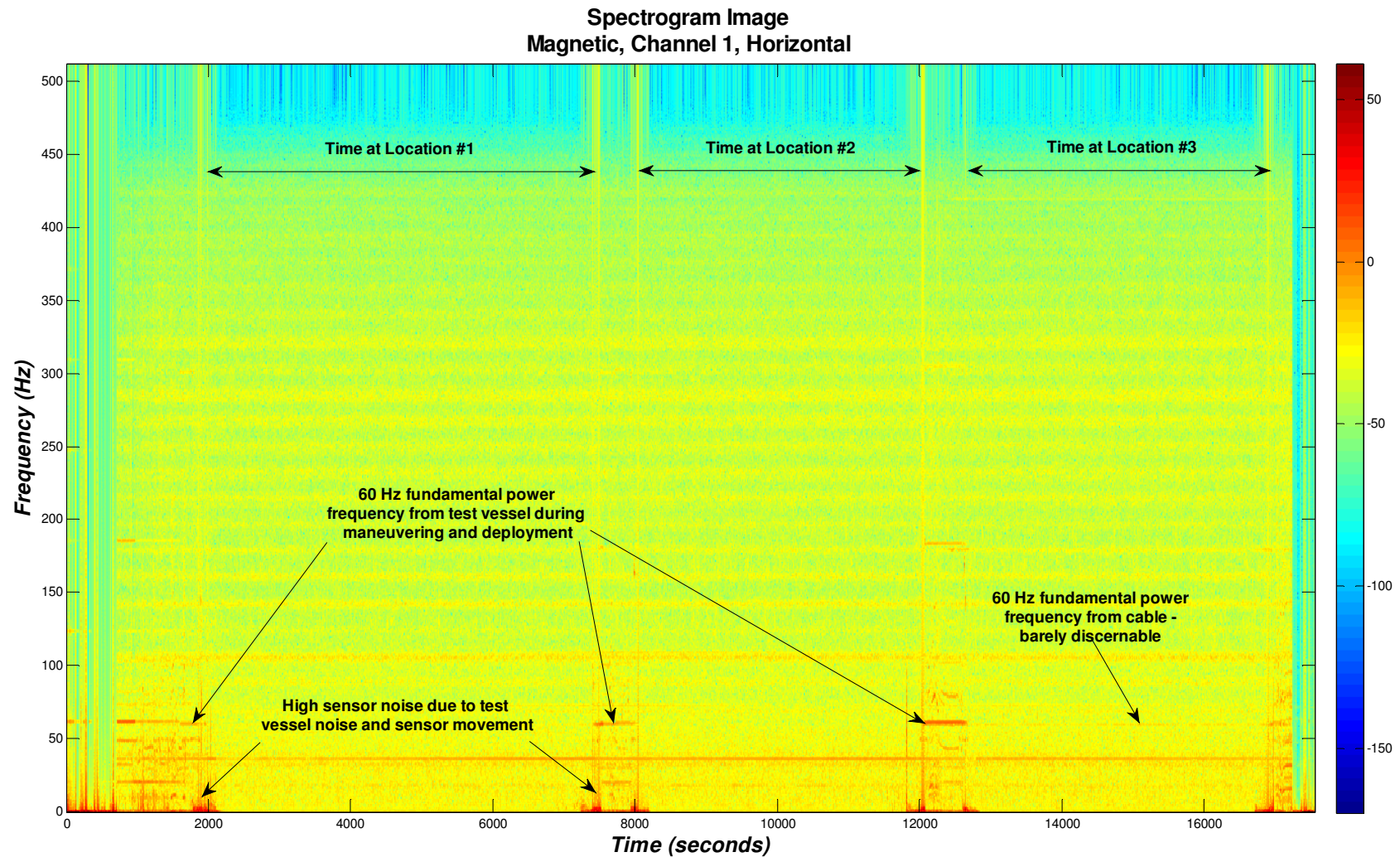


Figure 12 - B-Field Spectrogram Image, Sensor M1, Horizontal

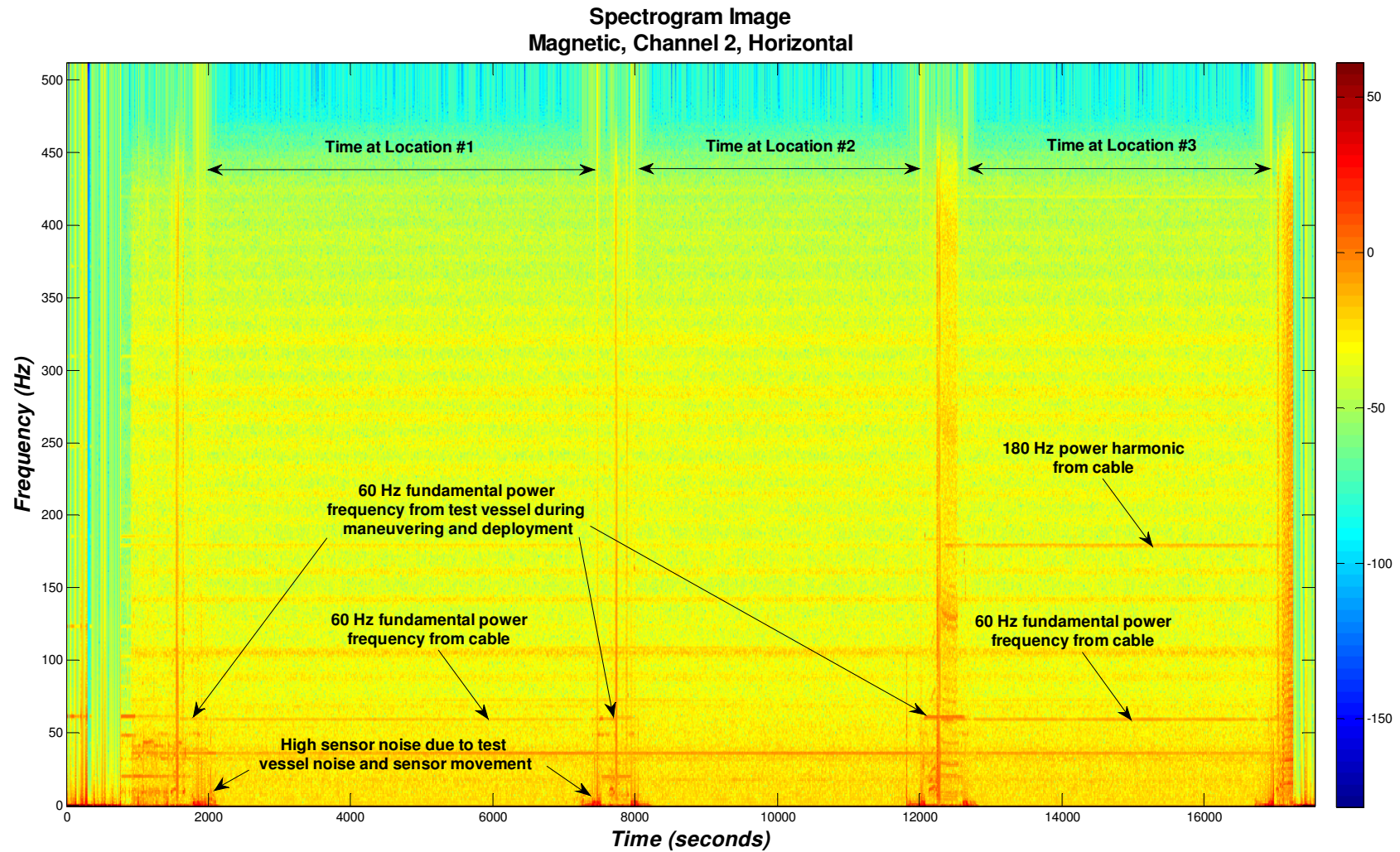


Figure 13 - B-Field Spectrogram Image, Sensor M2, Horizontal

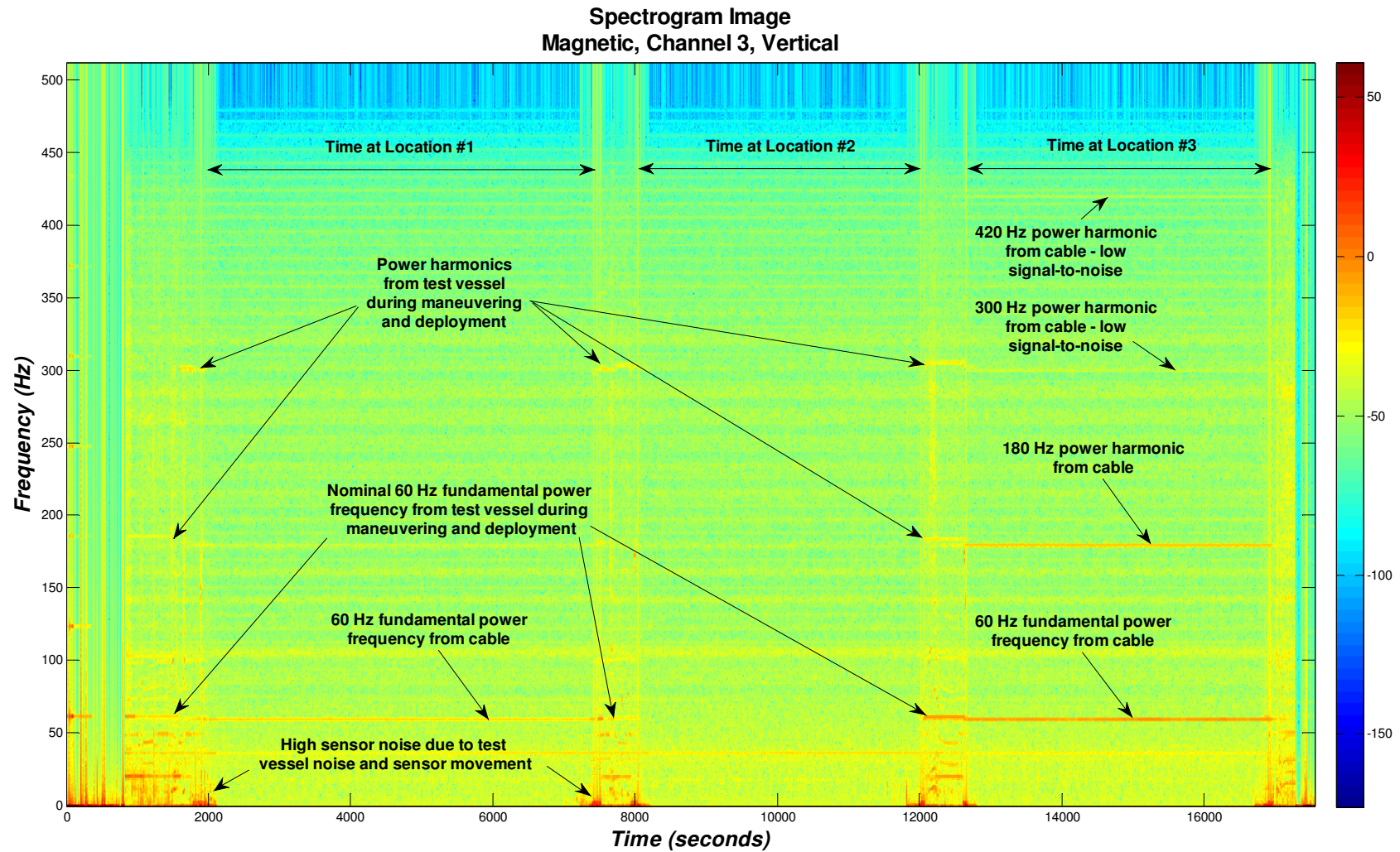


Figure 14 - B-Field Spectrogram Image, Sensor M3, Vertical

This is seen best by comparing Figure 14 (magnetic B-field in the vertical direction) to Figure 12, wherein the odd-harmonic power frequencies at 60, 180, 300, and 420 Hz are strongly evident in the vertical data, and are notably quiet in channel M1 (horizontal) data. Some signals are seen in Channel M2 (also horizontal magnetic) at 60 and 180 Hz, indicating that some magnetic energy was nonetheless detected in this dimension. Transient energy was evident during periods of recovering and repositioning the probe, underscoring the need to have a stable measurement platform to minimize system noise while taking measurements. Magnetic energy is easily induced on the sensors when they are moved with respect to the Earth's magnetic field, which can overload the inputs to these ultra-sensitive devices.

5.2 Spectral Analysis

In addition to time-frequency analysis, narrowband spectra were also computed using one-second integration periods using 1024 point fast-Fourier transforms to provide a 1 Hz equivalent noise bandwidth (spectrum level). Nominal signal-to-noise (SNR) values were computed and logged once per second during the measurement period for all measurement channels. This technique compared the peak tonal amplitudes to the amplitude of the spectral continuum adjacent to each tonal, in terms of a decibel ratio. SNR ratios greater than 10 dB indicate a strong signal not influenced by background (ambient) or system noise floor. SNR between 3 and 10 dB are considered to be influenced by background noise, and thus resultant amplitudes could be affected by local noise. Data with computed SNR values less than 3 dB are not provided, since these values were dominated by local noise affects, and did not represent accurate measured values. Figure 15 shows representative results of the magnetic (B-field) sensor in the vertical orientation (Sensor M3) at 60 Hz. Measurement locations are annotated on the figure. Highest SNR values were noted at location #3, closest to the cable, with typical SNR values greater than 30 dB. High SNR (>18 dB) was also noted at Location #1. Average SNR at location #2 were less than 3 dB, indicating that 60 Hz signals at this location and orientation combination were not substantially present above the background levels. Comparing these results to the visual spectrogram images (see Figure 14), it is evident that 60 Hz was not observed in the vertical direction at Location #2 approximately 500 meters away from the cable.

As expected, both electric and magnetic signatures at the fundamental power frequency (line voltage, 60 Hz) and higher order odd-harmonics (180 Hz (3x 60 Hz), 300 Hz (5x 60 Hz), and 420 Hz (7x 60 Hz)) from the energized cable were stronger near the cable (see representative narrowband spectrum in Figure 16). Signal amplitude diminished in locations away from the cable location.

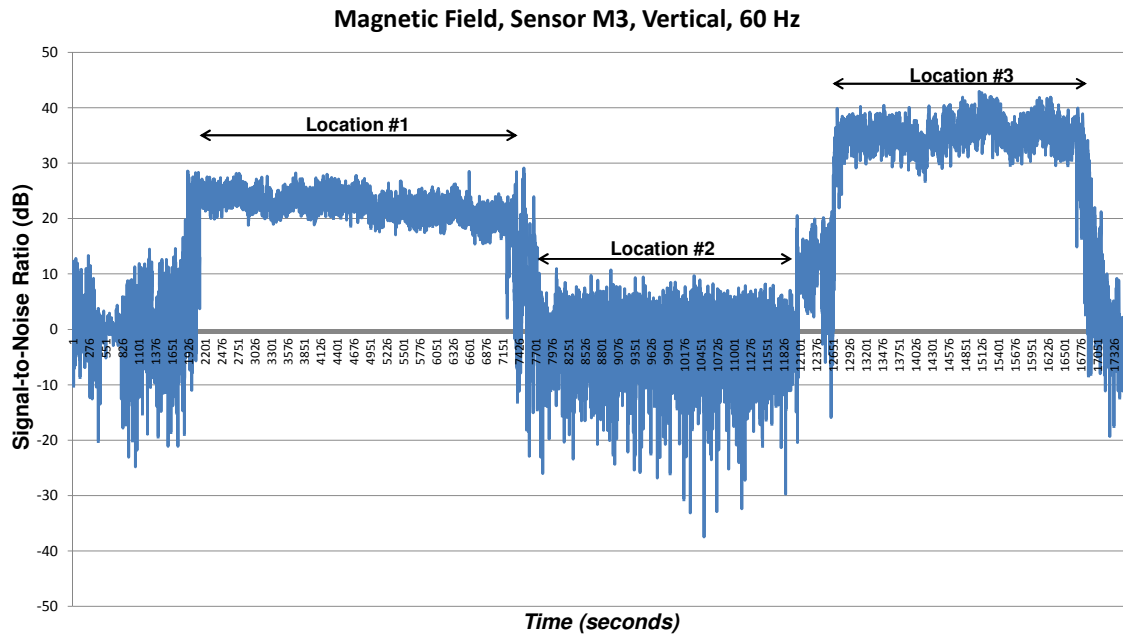


Figure 15 - Representative Signal-to-Noise Analysis, Magnetic Spectra, 60 Hz

Electric field strength at Location #2 were not readily measured using spectral processing, although 60 and 180 Hz tonals at both Locations #1 and #3 were strong, and 300 and 420 Hz tones were also measured at Location #3 within 75 meters of the cable. At distances greater than 50 meters from the cable, maximum E-field levels at 60 Hz were observed at 2 microvolts/meter ($\mu\text{V/m}$) or less. Longer integrations (up to 60 minutes) are possible to reduce the effective noise floor due to processing gain, but this was not analyzed since the 60 Hz power frequency and related harmonics were readily apparent in the data set at a 1 Hz bandwidth (spectrum level).

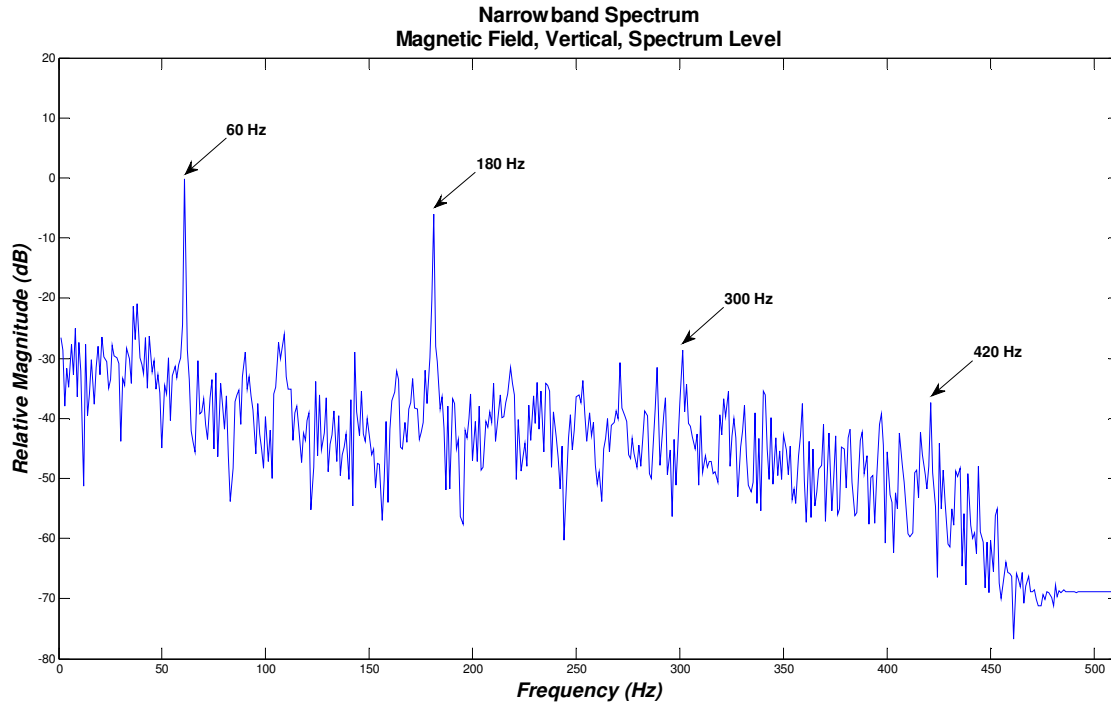


Figure 16 - Representative B-field magnetic spectrum, vertical, 1 Hz bandwidth

Table 3 presents the E-field AC power frequency summary for odd harmonics of 60 Hz at each of three measurement locations.

Table 3 - Electric Field Summary, AC Power Frequencies, Spectrum Level

Frequency (Hz)	Magnitude Location #1 ($\mu\text{V/m}$)	SNR (dB)	Magnitude Location #2 ($\mu\text{V/m}$)	SNR (dB)	Magnitude Location #3 ($\mu\text{V/m}$)	SNR (dB)
60	0.67	8	--	<3	1.98	18
180	0.26	3	--	<3	1.60	19
300	---	<3	--	<3	0.23	3
420	---	<3	--	<3	0.17	3
Approximate distance to AC power cable: Location #1: 150 to 200 meters Location #2: 400 to 500 meters Location #3: 50 to 75 meters Magnitude is computed as vector sum of horizontal and vertical components.						

Table 4 presents the magnetic B-field summary of measured power frequencies. As with the electric field data, field strength was directly related to the distance from the probe to the energized cable, as expected. A relatively weak 180 Hz frequency was measured at Location #2, which was not appreciably above the background level. 60 and 180 Hz magnetic field energy was easily observed at both Locations #1 and #3 (within 200 meters of the cable), with good signal to noise ratios, indicating a significant margin above the background noise levels at those frequencies and locations. Maximum levels were measured at Location #3 at 60 Hz, at 0.13 nT, but no power frequencies were seen at Location #2, which was estimated to be 400 to 500 meters from the energized cable. For reference, the earth's total magnetic field is approximately 52,000 nT (.000052 Tesla, or .52 Gauss) along the Oregon coast.¹

Table 4 - Magnetic Field Summary, AC Power Frequencies, Spectrum Level

Frequency (Hz)	Magnitude Location #1 (nT)	SNR (dB)	Magnitude Location #2 (nT)	SNR (dB)	Magnitude Location #3 (nT)	SNR (dB)
60	0.04	10	---	<3	0.13	20
180	0.02	12	---	<3	0.07	24
300	---	<3	---	<3	0.01	3
420	---	<3	---	<3	0.01	9
Approximate distance to AC power cable: Location #1: 150 to 200 meters Location #2: 400 to 500 meters Location #3: 50 to 75 meters Magnitude is computed as vector sum of horizontal and vertical components.						

6. ACTIVE SOURCE VERIFICATION DEPLOYMENT

In addition to evaluating the prototype probe for energized and background noise measurements, the probe was deployed in Newport Bay, Oregon in July 2, 2010 to test the probe's magnetic capability to sense a low-frequency active EM signal on a submerged sewage pipe in the bay. The motivation for the test was to geo-locate the pipeline to in support of planned construction of a new pier in Newport. Although OWET allowed use of the probe as a test-of-opportunity of the

¹ <http://www.ngdc.noaa.gov/geomagmodels/IGRFGrid.jsp>

prototype in an active source scenario, work activities for this test were not funded by OWET. Personnel from OSU (Dr. Adam Schultz and Tristan Peery) and SAIC (Michael Slater) provided technical support during the test period.

6.1 Methodology

A buried and submerged sewage pipe and adjacent metallic conduit was energized with a 256 Hz square wave using a terrestrial geophysical transmitter provided by Zonge. The transmitter was grounded to the pipeline on shore, and a ground electrode was located in a position defining a right angle to the between the ground point and the presumed pipeline direction. The probe was able to detect the transmitted energy at the fundamental frequency of 256 Hz, and using vector properties of the magnetic field sensed by the probe, the magnitude of the vertical magnetic field at various locations could be mapped. The pipeline was buried under approximately 15 meters of sediments in water 15 meters deep.

6.2 Deployment

The probe was staged and assembled near the pier, and then transported to the deck of a small tug outfitted with an A-frame. The data recorders were started, and the tug maneuvered to each location of interest. The probe was lowered to the bottom for a series of nominal five-minute periods, picked up, and moved to the next location.

6.3 Data Analysis

Data acquired during the Newport Bay active source testing were processed using time-frequency analysis in the same manner described for the background data analysis. A spectrogram image of the magnetic sensor in the vertical orientation is shown in Figure 17. Frequency is shown along the left axis, and time (in seconds) runs from left to right. A total span of approximately three hours is shown. Red color in the spectrogram image on the left and right sides represent high signal levels due to sensor motion while the probe was being transported to and from the pier to the measurement site. During the measurement period, the probe was lowered to the bottom in approximately 15 meters of water, and then recovered, moved to the next position, and repeated. Data were acquired continuously throughout this period. A strong signal at 256 Hz due to the source on the pipeline conduit was clearly evident during the measurement period.

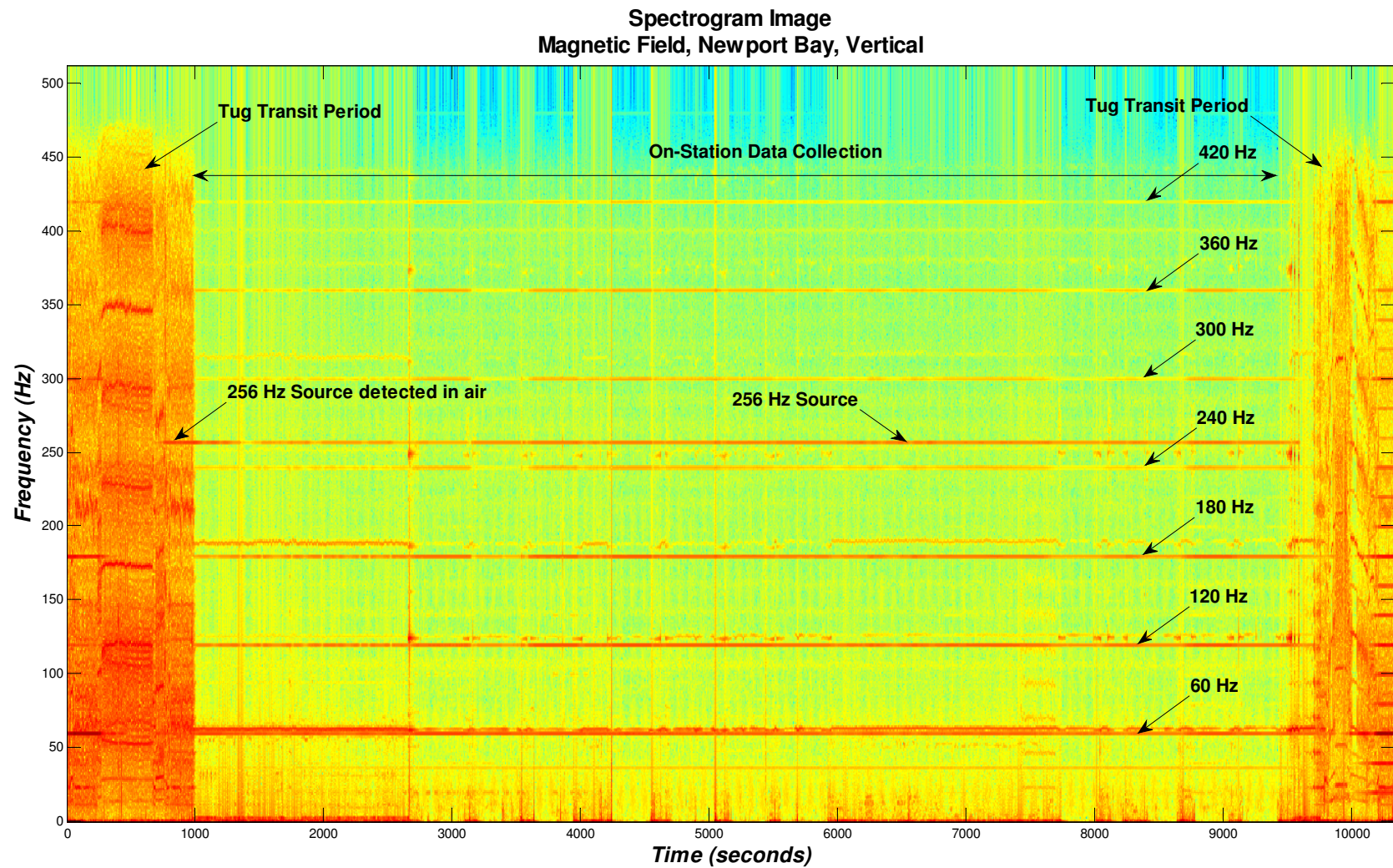


Figure 17 - B-Field Spectrogram Image, Sensor M3, Vertical

A narrowband spectrum (1 Hz bandwidth) was computed at one representative location to demonstrate the ability of the probe to sense and quantify measured signals (see Figure 18). The signal level at 256 Hz had sufficient strength to be observed with the probe in-air on the deck of the tug (see left hand side of chart) prior to placing the probe in the water. From the perspective of calibrated measurements, this observation is not very useful, however, this result does significantly demonstrate that the long-distance propagation of the "air-wave" component of the EM fields can extend the influence of EMFs from the generation source as that energy propagates along the air-sea interface. A similar effect is also possible on the sea-bottom interface due any resistive components of the underlying sub-sea strata, and points to the critical need to consider the specific site geology and physical layout when predicting EM fields in potential wave energy sites. In other words, simplified models with infinitely deep conductive ocean assumptions do not adequately address this affect.

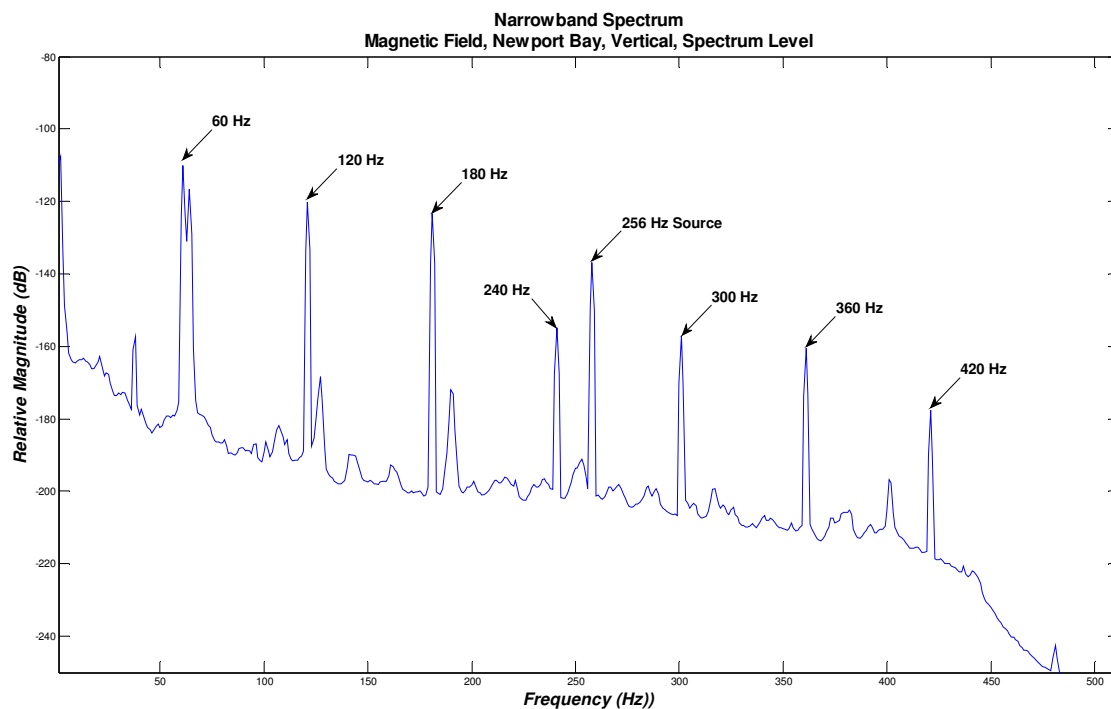


Figure 18 - Representative B-field magnetic spectrum, vertical, 1 Hz bandwidth

Measured levels in the water exhibited over 70 dB of signal-to-noise compared to the background levels. 60 Hz even and odd harmonics were clearly seen in the data from 60 Hz to 420 Hz, and relative signal levels were high relative to the background noise. The specific source for the power frequency signals was not immediately evident, but Newport Bay is a populated area, with a number of nearby commercial sources of power, including distribution lines, that could cause electrical power frequency emanations in the vicinity. It should be noted that similar effects may be observed at potential wave energy sites, especially those located adjacent to populated areas or those with power generation, distribution, or transmission features.

A magnitude-position analysis was prepared to determine the relative magnitude of the field relative to a fixed source as a function of position. Figure 19 shows the results of the vertical dimension of the B-field at 256 Hz. Periods of valid data collected are easily seen as “flat spots” in the chart, which represent periods during which the probe was stable on the bottom of the bay, resulting in a stable measurement of the source magnitude. As the physical location of the probe was changed, changes in magnitude were noted, seen as different relative magnitudes in the figure.

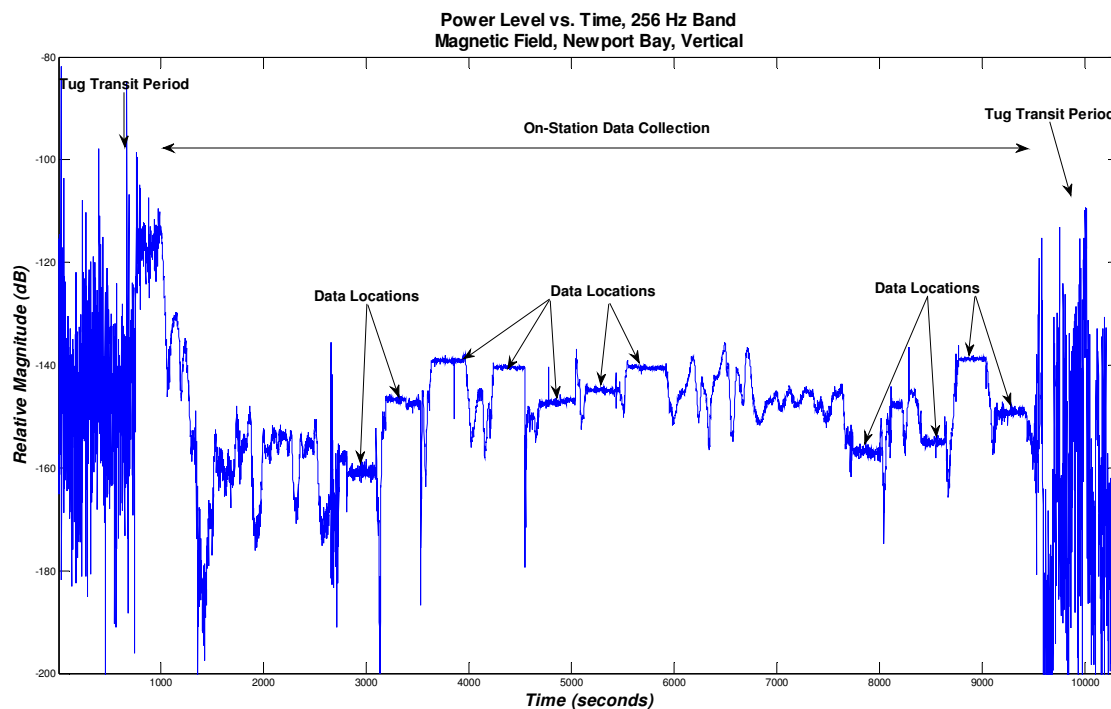


Figure 19 - B-field relative magnitude, vertical, 256 Hz band (1 Hz bandwidth)

7. DATA SUMMARY

The prototype probe effectively demonstrated the ability to sense and record wideband electric and magnetic field data underwater. Furthermore, in the presence of an energized AC submarine power cable, specific signatures emanating from an energized cable were assessed. Data analysis showed that the measurements were able to quantify background and energized cable noise, and that power frequencies could be measured at distances of 150 meters or more, even though the cable-of-opportunity measured was carrying less than 10 amps of current. Practically speaking, submarine power export cables would be carrying 10 to 100 times more electrical current, thus creating EM signatures that would likely be measureable over a larger distance from the cables or WEC devices than observed during the prototype test. Background levels were very low in the absence of power cable noise. Use of extremely low noise preamplifiers in the electric field sensors would be able to further reduce the noise floor of the probe in such cases where an extremely quiet background environment is expected. It was clear from handling of the sensing equipment that stationary probes were required to assess background noise. Motion of electrical field sensors underwater can induce spurious E-fields at the input of the data recorder. In addition, motion of the induction coil style magnetic sensors in the Earth's magnetic field can saturate the coil such that measured data could become clipped and unusable. Any motion by the probe during measurement periods will introduce noise and reduce the ability to sense background levels.

Data acquired in Newport Bay showed that energized sources could be detected and measured. This same data set also showed that 60 Hz noise and higher frequency harmonics (e.g. 120 Hz, 180 Hz, etc.) were prominent, but were due to one or more interfering noise sources, which could pose data interpretation difficulties at potential wave sites adjacent to power generation, distribution, or transmission facilities. That is to say, true background levels at power frequencies may be difficult to assess in populated areas where 60 Hz is somewhat ubiquitous, or if the local underlying geology supports efficient propagation into the surrounding environment.

8. DISCUSSION

Three primary objectives of this study were to demonstrate the reliability, affordability, and repeatability of acquiring EM signatures in the near-shore marine environment. The project's success in achieving these objectives is assessed in the following sections.

8.1 Measurement Reliability

Measurement reliability implies that signatures can be obtained when required, and in a manner that provides valid results. The prototype instrument demonstrated that valid electric and magnetic fields could be accurately assessed over a wide range of frequencies commonly found in the marine environment. On two separate deployments, wideband E- and B-field data were successfully sensed and recorded on multiple high-resolution channels, and the recordings persisted without issue over the planned measurement periods. As part of this demonstration, it was shown that magnetic and electric fields were detected in the vicinity of energized power cables, measured with a reasonable degree of precision as demonstrated by the laboratory calibration results, and accurately monitored over a period of time in multiple locations.

8.2 Measurement Affordability

The prototype probe was assembled using a combination of custom and commercially available equipment and supplies. The recording system and magnetic sensing components were adapted from a terrestrial geophysical application, and packaged to successfully operate in the marine environment at depths of up to 250 feet. Electric field sensors were fabricated in a laboratory environment with commonly available materials, again, following the basic technical approach used in the terrestrial geophysical exploration industry. A market survey for integrated wideband marine EM measurement equipment revealed that some components were available for EMF measurement, but the cost for an off-the-shelf integrated measurement solution was cost prohibitive, with vendors generally focusing on petroleum exploration and military markets. Hardware costs to replicate the prototype probe were found to be less than one-third the cost of commercial integrated systems, demonstrating that excellent progress was made to achieve the measurement affordability objective. The prototype probe was shipped via common carrier motor freight and pickup trucks, staged within a few hours, and deployed and retrieved using modest vessels, including local fishing vessels or working craft.

8.3 Measurement Repeatability

Calibration methodologies for EM measurements were developed and demonstrated using the prototype probe to obtain accurate signature measurement at different times and locations. In general, the calibration processes developed use commonly available bench top electrical equipment to verify sensor and recording integrity with traceability to NIST standards, and thus provides the basis for measurement repeatability from location-to-location, and at the same location over a long time horizon. Rigorous calibration methodologies are essential for comparison of data from different measurement sites, or by using different measurement equipment. Measurements and calibrations made with the prototype probe were shown to follow robust sensor and recording system calibration protocols. Our use of standard FFT processing techniques, including the application of standardized spectral processing bandwidth (e.g. spectrum level reporting of measured levels) encourage the adoption of de-facto standards to directly compare results at multiple sites or measurements made at different locations and periods of time using a common frame of reference.

In summary, three objectives of the study were achieved and demonstrated by use of the prototype EM probe system. Modeling, calibration, measurement, and processing protocols and techniques identified within this study serve to advance the science of marine EM measurements in coastal waters, and promote a standardized methodology that is reliable and repeatable.

9. CONCLUSIONS AND RECOMMENDATIONS

9.1 Summary Observations

At the most basic level, electric and magnetic fields are part of our everyday lives, and emanate from both natural (solar, planetary, geological, and oceanic processes) and man-made (electrical generation and transmission equipment, appliances, machinery) sources. EM theory predicts that such fields are expected to exist in air, underwater, and within the earth and seabed, with extremely low electric field levels in the ocean due to the electrical conductivity of the water which serves to substantially attenuate any E-field values compared to in-air conditions. Magnetic conditions are significantly affected by the varying seawater and geologic conditions

along the coast. In particular, B-field propagation is directly impacted by the water column, as well as by the air/sea interface and the sub-seafloor electrical resistivity structure. This study demonstrated that such fields do indeed exist in the near-shore marine environment, and can be accurately quantified with a reasonable investment of care and ingenuity in instrumentation and understanding of the physical characteristics of the measurement problem. Naturally occurring background measurements can be made in the marine environment, and furthermore, reasonably precise assessments can be made of submerged AC power cables.

9.2 Application of the Technology

This study laid the groundwork for what is both known and unknown in the science of reliable, affordable, and repeatable marine EM measurements. Although few measurements exist in real-world shallow water environments, available theories and supporting literature provide ample evidence of EM field generation and propagation behavior in this context. Use of the prototype probe and the measurement approach in general can provide site assessment capabilities and meet EMF quantification requirements. As required, application of this equipment and generalized measurement approach can also be used to provide the physical baseline for on-going monitoring of potential wave energy sites. In addition, this equipment and related calibration and measurement techniques can support mesocosm or other behavioral and habitat experiments with marine species to best inform and correlate with potential or observable impacts of introducing power generating or transmission sources into the marine ecosystem. EMF propagation is strongly related to local physical conditions, and in-situ observations would provide realistic interpretations to biological responses.

9.3 Additional Technical Recommendations

As a result of a literature review, it became clear that specific published effects to marine species with respect to power frequencies from submarine cables were lacking. A fair bit of research has been published on effects to elasmobranchs (sharks and rays), and to a lesser degree information was available on turtles, but very little information was found on marine mammals, other fish species (including sturgeon and salmonids) or benthic organisms. Application of equipment and techniques documented within this study could easily be adapted to provide

repeatable, quantifiable EM field data to ensure that observable conclusions are based on valid data sets.

Recommendation: Conduct additional biological study to better understand and quantify observed effects to biota from man-made EMF. Apply equipment and techniques developed in this study in support this of biological research.

Due to the limited scope of the study, the long-term temporal variability of naturally occurring EM fields was not quantified in terms of range or extent. In terms of daily, monthly, or even seasonal variations, no conclusions were drawn as to how much environmental factors could change in a given location. Because man-made sources such as energized power cables are well known and quantified, however, it is reasonable to assert that emanations from operational cables can be estimated and monitored in real-time. Such parameters are a function of cable physical design factors, installation geometry, local geology or physical conditions (weather, salinity), and operational characteristics (e.g. applied voltage, applied current, and relative phase in the case of multi-phase cables). Longer term monitoring or periodic sampling would provide better insight into the naturally occurring environment.

Recommendation: Conduct long-term monitoring with energized cables. As part of monitoring, collect electrical and physical data to correlate measured levels to physical phenomena.

Modeling and predictions of E- and B-field strengths used in this study relied on homogenous, simplified approaches, and did not involve the use of specific, localized geology to predict unique EM propagation behaviors at specific locations. Two methods are available to perform this activity:

1. preparation of a three-dimensional model of the local geology and postulated wave energy site layout to predict the EM fields generated; and
2. acquisition of in-situ measurements of the environment before, during, and after such an installation.

From a cost and predictive standpoint, the modeling approach coupled with in-situ measurements to “spot check” results would provide useful results during the planning stages of site evaluation,

and would not require extensive field work to fully map EM fields in the local environment. Literature results highlighted in this study revealed that the strength and orientation of electromagnetic fields depends strongly on the water depth and conductivity, the geometry, and electric current density of the electric power generation and transmission lines, and on the geometry and electrical resistivity structure of the seabed and sub-seabed geologic formations. The presence of electrically resistive formations in the shallow sub-seabed can act as a waveguide that can channel EMFs to greater distances from their point of generation than would be indicated by simpler conceptual models. The air-sea interface also affects the long distance propagation of EMFs, a consideration that is not factored in the basic propagation models. Development of a detailed modeling protocol was beyond the scope of this study, but this capability currently exists at Oregon State University's Geoelectromagnetic Laboratory, the home of the National Geoelectromagnetic Facility (NGF).² NGF has developed a high performance computing capability necessary to calculate realistic EMF propagation in complex three dimensional submarine settings, for near-shore and deeper water environments, including calculations that can extend EMF propagation on land as well as at sea. Advancement of this technology to generate predictions of EMFs would serve to reduce the amount of effort and expense to conduct field measurements, and hence, encourage development of marine energy power sources.

Recommendation: Evaluate and improve existing modeling capabilities with measured data at wave energy sites. Consider performing this activity while concurrently monitoring energized cables along Oregon's coast.

ACKNOWLEDGEMENT

The authors gratefully acknowledge the support of the Oregon Wave Energy Trust, the OWET Board of Directors, and in particular, the Mr. Jason Busch, OWET Executive Director, for enabling this research as an important piece of marine renewable energy technology.

² ngf.coas.oregonstate.edu

APPENDIX A – ACRONYMS

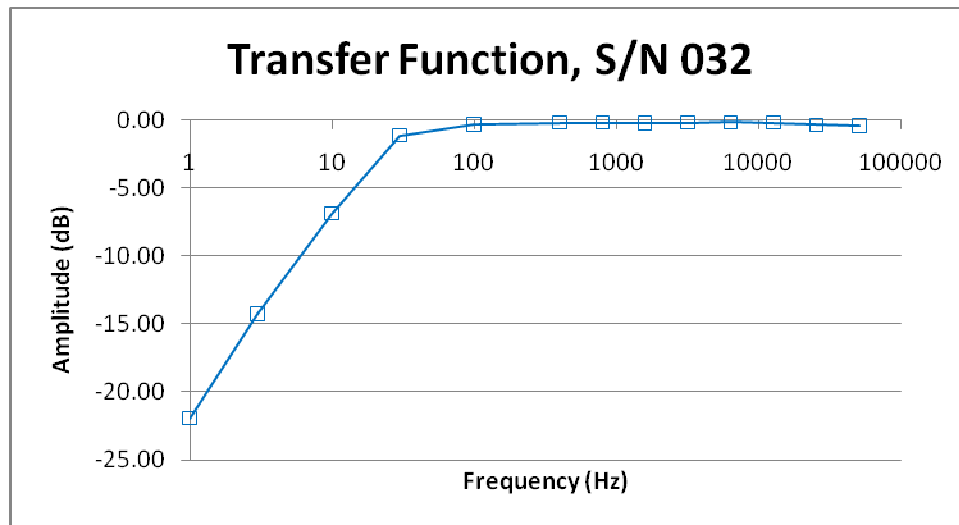
1-D	one dimensional
2-D	two dimensional
3-D	three dimensional
ASW	anti-submarine warfare
B-field	magnetic field
CA	California
CGS	centimeter-gram-second
CMACS	Centre for Marine and Coastal Studies
COWRIE	Collaborative Offshore Wind Research into the Environment
DoI	Department of Interior
EA	Environmental Assessment
E-field	electric field
EIS	Environmental Impact Statement
EM	electromagnetic
EMF	electromagnetic field
fT	femto Tesla
Hz	Hertz, cycles per second
kHz	kilo Hertz
μT	micro Tesla
μV	micro volts
mHz	milli Hertz
mT	milli Tesla
mV	milli volts
MKS	meter-kilogram-second
MMS	Minerals Management Service
NIST	National Institute of Standards and Technology
nT	nano Tesla
nV	nano volts
ODFW	Oregon Department of Fish and Wildlife
OPT	Ocean Power Technologies
OR	Oregon
OWET	Oregon Wave Energy Trust
PSD	Power spectral density
pT	pico Tesla
SEMC	Seafloor Electromagnetic Methods Consortium
SI	International System of Units
SIO	Scripps Institute of Oceanography
UK	United Kingdom
US	United States
WA	Washington
WEC	Wave Energy Converter

APPENDIX B – PROBE CALIBRATION LOGS

Magnetometer Calibration Data Log

Unit Serial Number: 032 Date: 9/8/2010
 Calibration Resistor: 988 ohms Calibrated by: M. Slater
 Sensitivity 0.1 V/1nT

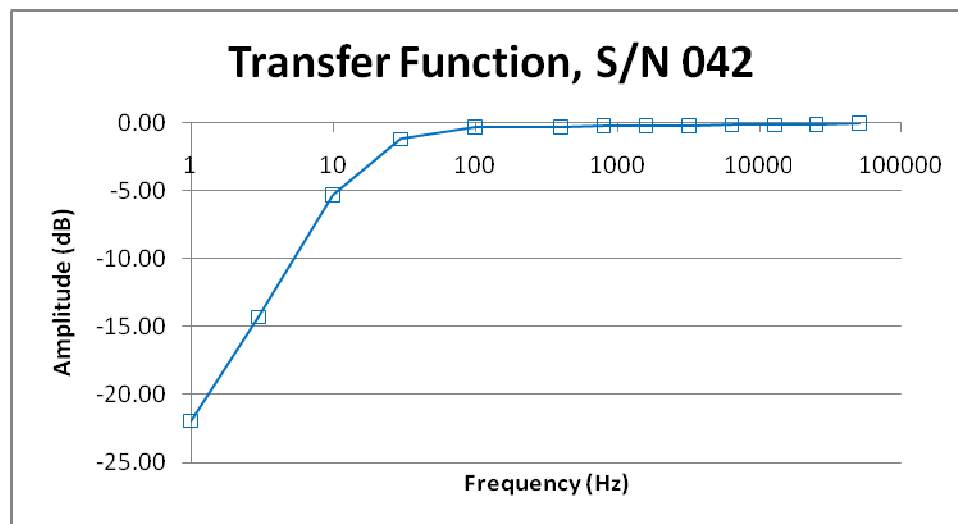
Input Frequency (Hz)	Coil Current (μArms)	Coil Field Strength (nT)	Calculated Output (dBVrms)	Measured Output (dBVrms)	Transfer Function (dB)
1	168	8.31	-1.606	-23.56	-21.95
3	200	9.89	-0.092	-14.36	-14.27
10	200	9.89	-0.092	-6.97	-6.88
30	201	9.94	-0.049	-1.18	-1.13
100	201	9.94	-0.049	-0.390	-0.34
400	201	9.94	-0.049	-0.24	-0.19
800	201	9.94	-0.049	-0.24	-0.19
1600	201	9.94	-0.049	-0.29	-0.24
3200	201	9.94	-0.049	-0.24	-0.19
6400	200	9.89	-0.092	-0.25	-0.16
12800	200	9.89	-0.092	-0.29	-0.20
25600	202	9.99	-0.005	-0.36	-0.35
51200	203	10.04	0.037	-0.37	-0.41



Magnetometer Calibration Data Log

Unit Serial Number: 042 Date: 9/8/2010
 Calibration Resistor: 988 ohms Calibrated by: M. Slater
 Sensitivity 0.1 V/1nT

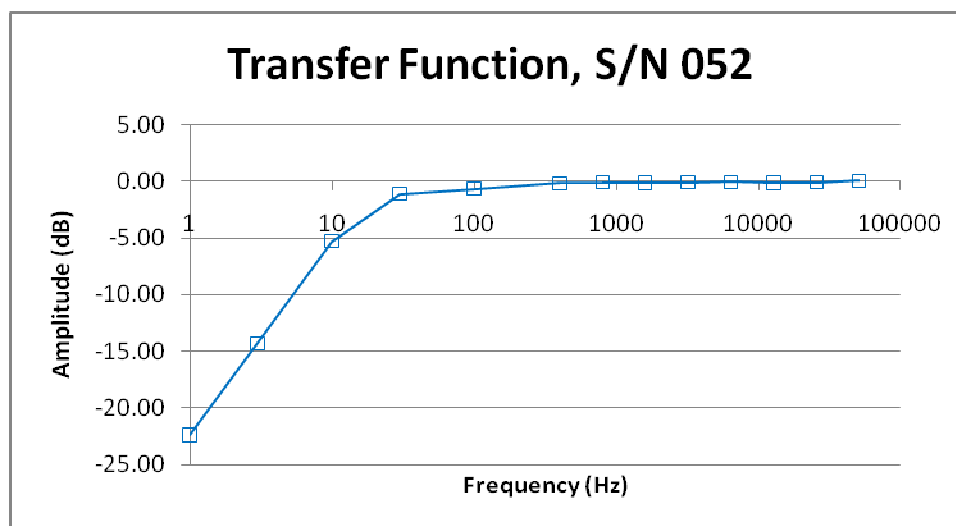
Input Frequency (Hz)	Coil Current (μ Arms)	Coil Field Strength (nT)	Calculated Output (dBVrms)	Measured Output (dBVrms)	Transfer Function (dB)
1	201	9.94	-0.049	-21.99	-21.94
3	201	9.94	-0.049	-14.35	-14.30
10	201	9.94	-0.049	-5.36	-5.31
30	201	9.94	-0.049	-1.25	-1.20
100	201	9.94	-0.049	-0.380	-0.33
400	201	9.94	-0.049	-0.36	-0.31
800	201	9.94	-0.049	-0.29	-0.24
1600	201	9.94	-0.049	-0.29	-0.24
3200	201	9.94	-0.049	-0.29	-0.24
6400	200	9.89	-0.092	-0.27	-0.18
12800	200	9.89	-0.092	-0.26	-0.17
25600	200	9.89	-0.092	-0.24	-0.15
51200	203	10.04	0.037	0.01	-0.03



Magnetometer Calibration Data Log

Unit Serial Number: 052 Date: 9/8/2010
 Calibration Resistor: 988 Ohms Calibrated by: M. Slater
 Sensitivity 0.1 V/1nT

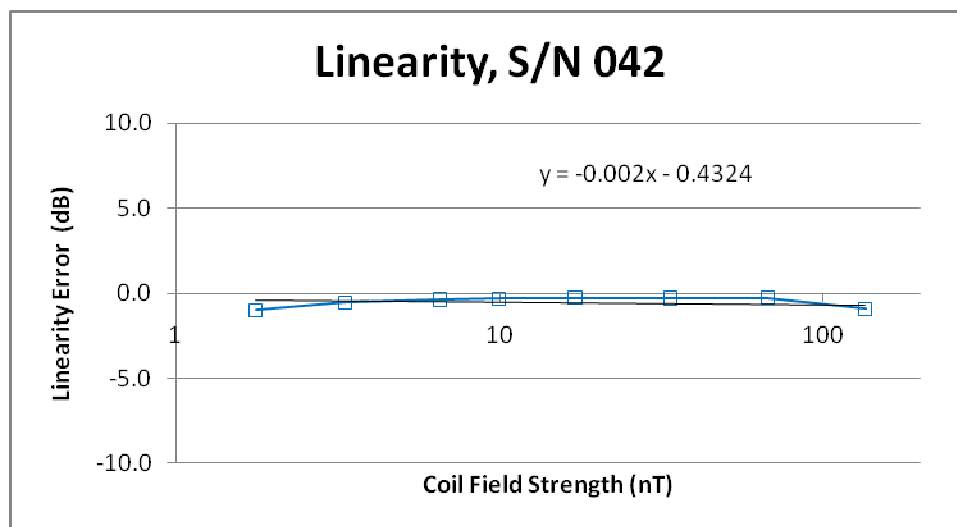
Input Frequency (Hz)	Coil Current (μ Arms)	Coil Field Strength (nT)	Calculated Output (dBVrms)	Measured Output (dBVrms)	Transfer Function (dB)
1	167	8.26	-1.658	-24.06	-22.40
3	201	9.94	-0.049	-14.36	-14.31
10	201	9.94	-0.049	-5.33	-5.28
30	201	9.94	-0.049	-1.15	-1.10
100	201	9.94	-0.049	-0.700	-0.65
400	201	9.94	-0.049	-0.23	-0.18
800	201	9.94	-0.049	-0.16	-0.11
1600	201	9.94	-0.049	-0.17	-0.12
3200	201	9.94	-0.049	-0.16	-0.11
6400	200	9.89	-0.092	-0.14	-0.05
12800	200	9.89	-0.092	-0.24	-0.15
25600	202	9.99	-0.005	-0.09	-0.08
51200	202	9.99	-0.005	0.04	0.05



Linearity Data Log

Unit Serial Number: 042 Date: 9/8/2010
 Calibration Resistor: 988 ohms Calibrated by: M. Slater
 Sensitivity 0.1 V/1nT

Input Frequency (Hz)	Coil Current (μ Arms)	Coil Field Strength (nT)	Calculated Output (dBVrms)	Measured Output (dBVrms)	Linearity Error (dB)
100	36	1.76	-15.083	-16.09	-1.01
100	67	3.33	-9.539	-10.08	-0.54
100	132	6.53	-3.701	-4.08	-0.38
100	201	9.94	-0.049	-0.38	-0.33
100	345	17.07	4.644	4.380	-0.26
100	682	33.74	10.563	10.28	-0.28
100	1363	67.43	16.577	16.3	-0.28
100	2725	134.82	22.595	21.66	-0.93



Noise floor of calibration environment: -75dBV/VHz, at 100 Hz, equivalent to 1.78 pT/VHz, or $\sim 10^{-12}$ T

APPENDIX C – REFERENCE DOCUMENTS

- (a) Slater, M.A., Schultz, A. (2009). “Electromagnetic field measurements: field sensor recommendations.” Oregon Wave Energy Trust, www.oregonwave.org
- (b) Webb, S. C., S. C. Constable, C. S. Cox, T. K. Deaton. (1985). “A Seafloor Electric Field Instrument.” Journal of Geomagnetic and Geoelectric Studies (Vol 37), pp. 1115-1129.
- (c) Petiau, Gilbert. (2000). “Second generation of Lead-Lead Chloride electrodes for geophysical applications.” Pure and Applied Geophysics (Vol. 157). pp. 357-382.
- (d) Slater, M.A. (2009). “Electromagnetic field measurements: instrumentation configuration.” Oregon Wave Energy Trust, www.oregonwave.org